Optical Arbitrary Waveform Generation and Characterization Using Spectral Line-by-Line Control

Zhi Jiang, *Student Member, IEEE*, Daniel E. Leaird, *Senior Member, IEEE*, and Andrew M. Weiner, *Fellow, IEEE, Fellow, OSA*

***Abstract*—This paper demonstrates optical arbitrary waveform generation (O-AWG) and its characterization using spectral line-by-line control with high-resolution grating-based pulse shapers. Such integrated capabilities are the enabling techniques for high-fidelity O-AWG.**

***Index Terms*—Frequency comb, mode-locked laser, optical arbitrary waveform generation (O-AWG), pulse characterization, pulse shaping.**

I. Introduction

MODE-LOCKED lasers generate periodic trains of ultrashort pulses that are characterized in the frequency domain by an evenly spaced series of discrete spectral lines (an optical frequency comb), with the frequency spacing equal to the pulse repetition rate. Spectral lines and their stabilization in mode-locked lasers have recently played a critical role in the progress of optical frequency metrology and optical carrier–envelope phase control [1]. Meanwhile, pulse-shaping techniques, in which intensity and phase manipulation of optical spectral components allow the synthesis of user-specified ultrashort pulse fields according to a Fourier transform relationship, have been developed and widely adopted [2]. With the possibility to extend pulse shaping to independently manipulate the intensity and phase of individual spectral lines (line-by-line pulse shaping), essentially arbitrary optical waveform generation can be achieved. Intuitively, a full control of individual spectral lines requires 1) frequency stabilized sources to generate stable spectral lines and 2) high-resolution pulse shapers to resolve and control individual spectral lines. Optical arbitrary waveform generation (O-AWG) that results from line-by-line pulse shaping, which is a combination of both enabling techniques, will serve as the basis for new applications and promises broad impact in optical science and technology. For example, we mention several possibilities within the context of communications. O-AWG can be used to generate return-to-zero (RZ) pulses with tailored pulsewidth and chirp, which is of particular interest for RZ format transmission, soliton systems, optical time-division multiplexing, and optical packet generation [3]. In many optical code-division-multiple-access (O-CDMA) systems, input ultrashort pulses are time-spread during the encoding process into lower intensity noise-like signals [4]. O-AWG can be used to generate such encoded signals with desired properties, such as longer code lengths, and in some cases, reduced fluctuations, to enhance system performance. O-AWG can also be used to obtain the optical driving signals for radio-frequency arbitrary waveform generation (RF-AWG) [5], which has the potential to impact fields such as ultrawideband (UWB) wireless communications and impulse radar. In addition to specific applications of O-AWG, line-by-line pulse shaping may also be useful in the context of spectral line stabilization and optical frequency metrology, because it is sensitive to the spectral line positions.

The recent advances of both enabling techniques are at a stage where spectral line-by-line pulse shaping can be pursued. From the perspective of frequency-stabilized sources, stabilization of the absolute frequency offset positions of the spectral lines of mode-locked lasers has recently been achieved [6]. The resultant optical frequency combs have led to enormous progress in precision optical frequency synthesis and metrology [7], [8]. Here, we will focus on the perspective of high-resolution pulse shapers that are able to resolve and control individual spectral lines. In contrast, past pulse shapers have generally manipulated groups of spectral lines rather than individual lines, which results in waveform bursts that are separated in time with low duty factor and which are insensitive to the absolute frequency positions of the mode-locked comb. This is primarily due to the practical difficulty of building a pulse shaper that is capable of resolving each spectral line for typical mode-locked lasers with repetition rates below 1 GHz. Group-of-lines pulse shaping is illustrated in Fig. 1(a), where $f_{\rm rep}$ is the repetition rate. Assuming that the pulse shaping occurs M lines at a time, the shaped pulses have maximum duration $\sim 1/(Mf_{\rm rep})$ and repeat with period $T = 1/f_{\rm rep}$. Accordingly, the pulses are isolated in time. In contrast, for line-by-line pulse shaping $(M = 1)$ as shown in Fig. 1(b), the shaped pulses can overlap with each other, which leads to waveforms that span the full time period between mode-locked pulses (100% duty factor). Waveform contributions arising from adjacent mode-locked pulses will overlap and interfere coherently in a manner sensitive to the offset of the frequency comb [9]. Such line-by-line control makes true O-AWG possible because the intensity and phase of each individual spectral line is fully controlled. Group-of-lines pulse shaping can be considered as

Manuscript received September 26, 2005; revised December 12, 2005. This work was supported by Defense Advanced Research Projects Agency (DARPA) under Grant MDA972-03-1-0014.

The authors are with the School of Electrical and Computer Engineering, Purdue University, West Lafayette, IN 47907-2035 USA (e-mail: zjiang@purdue.edu; leaird@purdue.edu; amw@ecn.purdue.edu).

Digital Object Identifier 10.1109/JLT.2006.874661

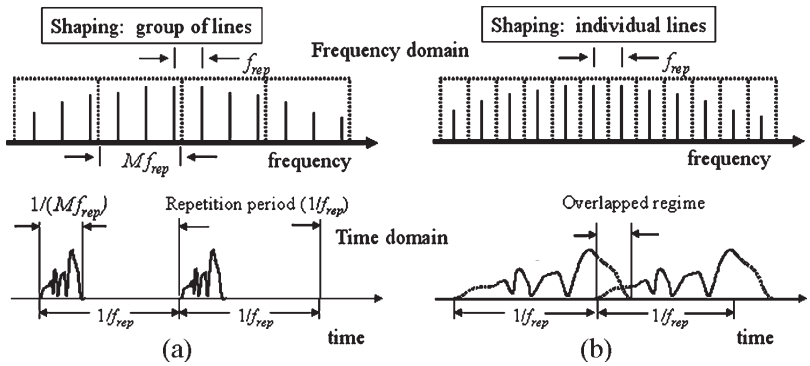

Fig. 1. Different pulse shaping methodologies. (a) Manipulating groups of lines. (b) Manipulating individual lines.

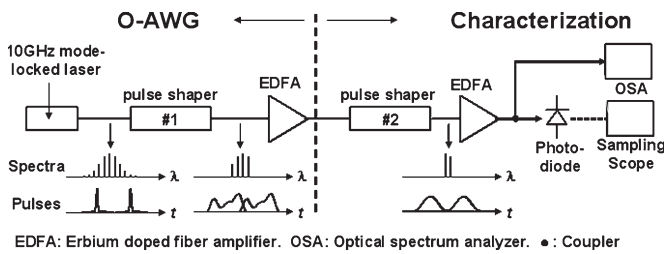

Fig. 2. Experimental setup for O-AWG and its characterization using spectral line-by-line control.

a special case of line-by-line pulse shaping. All group-of-lines pulse shaping results can be achieved using a line-by-line pulse shaper by simply applying identical intensity/phase on each group of lines. Previous efforts toward spectral line-by-line control utilized a hyperfine filter but were limited within a narrow optical bandwidth—the free spectral range of this device [10], [11]. Recently, we demonstrated spectral intensity/phase line-by-line pulse shaping [9] and thus O-AWG over a considerably broader band [12] based on high-resolution grating-based pulse shapers.

One immediate issue related to O-AWG is its characterization to ensure that the desired waveform has been generated correctly. Commercial high-speed photodiodes have bandwidths limited to $\sim$ 60 GHz, which is insufficient for most O-AWG measurements. Furthermore, the temporal phase information is lost because the photodiode is a square-law device. Various optical techniques have been developed to completely characterize the intensity and phase of optical pulses, which are based on the concept of spectrography [e.g., frequency-resolved optical gating (FROG)] [13], interferometry [e.g., spectral phase interferometry for direct electric-field reconstruction (SPIDER)] [14], and tomography [15]. Among the available possibilities, an interferometry-based method [16]–[18] is particularly appealing for the characterization of O-AWG-generated waveforms by spectral line-by-line pulse shaping because this method also relies on spectral line-by-line control. In this paper, we integrate the functionalities of both O-AWG and its characterization based on spectral line-by-line control as an enabling technology for high-fidelity O-AWG.

II. Experimental Setup

Fig. 2 shows our experimental setup, which includes the O-AWG section and the characterization section. In the O-AWG section, a home-built harmonically mode-locked fiber laser is used to produce near-transform-limited 3-ps (full-width at half-maximum) pulses at 1542.5-nm center wavelength with a repetition rate of 10.0 GHz. The frequency offset of the mode-locked comb is not actively stabilized; instead, we exploit the passive frequency stability of the mode-locked comb, $\sim$ 1 GHz over the time scale of our experiments (ten times below the comb spacing). This suffices for our experiments under typical laboratory environmental conditions without additional controls (e.g., temperature stabilization). The mode-locked laser is followed by a programmable pulse shaper [2] for O-AWG using spectral line-by-line pulse shaping. Erbium-doped fiber amplifiers (EDFAs) are used for loss compensation. In the characterization section, a second pulse shaper is used to filter only two spectral lines (this is monitored by an optical spectrum analyzer). The resulting cosine waveform (with a dc offset) from the beat of these two spectral lines is detected by a 50-GHz photodiode and measured by a sampling oscilloscope. The details of this measurement method can be found in [16] and will be briefly described later.

Spectral line-by-line control for O-AWG and its characterization is accomplished by high-resolution fiber-coupled Fourier transform pulse shapers in a reflective geometry [2], [9], [12]. To achieve line-by-line pulse shaping, great care is taken in the pulse shaper design to improve resolution. Fig. 3 shows the experimental apparatus for a line-by-line pulse shaper. For each pulse shaper, a fiber-pigtailed collimator and a subsequent telescope take the light out of the fiber and magnify the beam size on the diffraction grating. Discrete spectral lines making up the input short pulse are diffracted by the grating and focused by a lens. A fiberized polarization controller (PC) is used to adjust for horizontal polarization on the grating for high diffraction efficiency. A 2×128 pixel liquid crystal modulator (LCM) array with a polarizer on the input face is placed just before the lens focal plane to independently control both the amplitude and phase of individual spectral lines. A retroreflecting mirror at the lens focal plane leads to a double-pass geometry, with all the spectral lines recombined into a single fiber and separated from the input via an optical circulator. For the characterization pulse shaper, a slit can be used to replace the LCM as only two lines need to be selected. Actually, in our experiments, in addition to an LCM, a slit is used to assist in blocking unwanted lines when the contrast ratio of intensity modulation applied by the LCM is not sufficient. The parameters of both pulse shapers

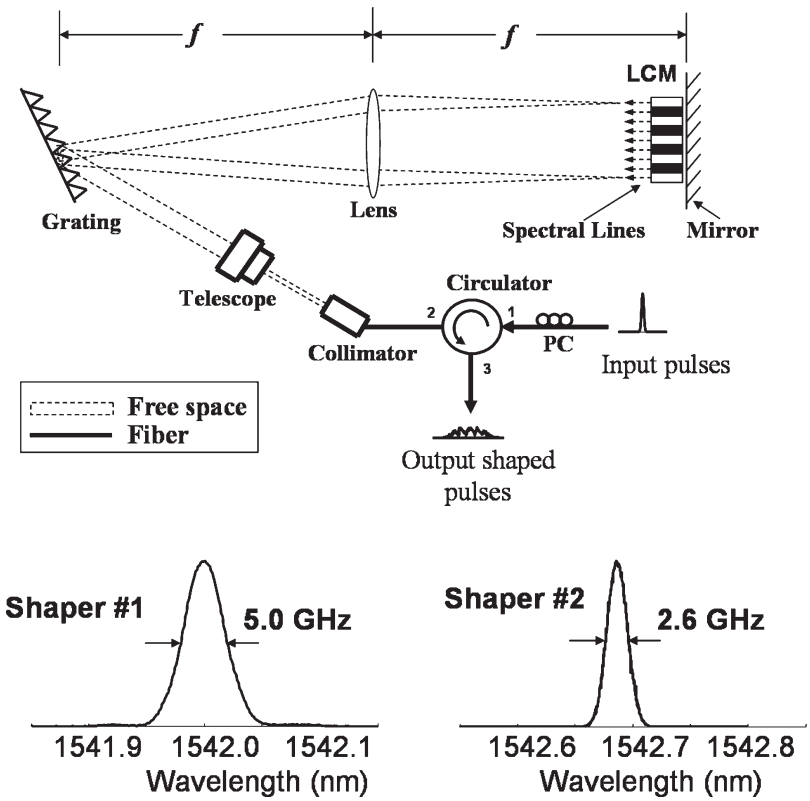

Fig. 3. Experimental apparatus of a line-by-line pulse shaper. The inset shows the measured 3-dB passband of 5.0 GHz (first pulse shaper—generation) and 2.6 GHz (second pulse shaper—measurement). LCM: liquid crystal modulator. PC: polarization controller.

TABLE I
PULSE SHAPER PARAMETERS

	Collimated beam diameter before grating (mm) *	Grating lines (/mm)	Lens focal length (mm)	Loss (dB) (including circulator)
Shaper #1	18	1100	750	12.0
Shaper #2	18	1200	1000	11.6

*: Beam diameter is defined as intensity decreases to $1/e^2$ of peak value

are listed in Table I. Using a narrow slit, the measured passband of the line-by-line pulse shapers has a minimum 3-dB passband width of 5.0 GHz and 2.6 GHz for the first (generation) and second (measurement) pulse shapers, respectively, as shown in the inset. Both pulse shapers have high resolution to afford line-by-line control at the $\sim$ 10-GHz laser repetition rate, which is appropriate for applications in optical communications. For accurate line-by-line control, the spectral line spacing of the mode-locked laser (the repetition rate) has to match the spatial spacing of the pixels (or integer multiple of the pixel spacing). This can be implemented by tuning the grating diffraction angle and/or tuning the repetition rate of the actively mode-locked fiber laser. Note that our line-by-line pulse shaper is finely adjusted to achieve zero dispersion [2], which is confirmed by negligible broadening for 3-ps pulses passing through the pulse shaper without spectral filtering. This is important for both pulse shapers. For the shaper in the O-AWG section, zero dispersion is important for accurate and known phase control (because, without filtering, input transform-limited pulses will remain transform-limited after the shaper). For the second pulse shaper (in the characterization section), zero dispersion ensures accurate phase characterization because no extra dispersion is inferred onto the waveforms to be measured.

The loss of the line-by-line pulse shapers in our current setup is higher than the loss of the relatively low-resolution fiber-coupled pulse shapers that we demonstrated before (4.0 dB) [4]. This mainly arises from the large size collimated beam after the telescope. The laser beam size makes it more difficult to focus the beam back into the 9-μm fiber mode after the pulse shaper, most likely due to lens aberrations (in the pulse shaper and in the telescope).

Note that the update speed of LCM is on the order of tens of milliseconds to $\sim$ 100 ms, which is limited by the liquid crystal relaxation time. Therefore, pulse-shaping experiments to date, including those reported here, are generally constrained to generate waveforms periodic at the repetition rate of the mode-locked laser source. To generate waveforms with different periods, the repetition rate of the laser should be changed. Accordingly, the pulse shaper design has to be modified to match the spectral line separation (the repetition rate of the laser). Alternatively, if a fast spatial light modulator technology capable of updating at the laser repetition rate were to become available, then aperiodic waveforms or waveforms with periodicities different than that of the input laser could be generated via appropriate reprogramming of the spatial light modulator on a pulse-by-pulse basis.

III. RESULTS AND DISCUSSIONS

First, the principle of pulse measurement is briefly sketched; further detail can be found in [16]. Considering any two spectral

lines selected by the pulse shaper at the characterization section, the field in the frequency domain can be expressed as

$$M(f) = \delta(f) + \sqrt{\beta} \cdot \delta(f - \Delta f) \cdot \exp(-j\theta) \quad (1)$$

where $\delta(\cdot)$ represents the impulse function, β and θ represent the relative intensity and phase between the two spectral lines, and Δf is the frequency spacing between two lines. Δf usually equals the mode-locked laser repetition rate $f_{\rm rep}$ if adjacent two lines are selected from the mode-locked laser. However, if there are lines missing between them, Δf would be an integer multiple of $f_{\rm rep}$. In the time domain, the intensity profile can be obtained by Fourier transform as

$$\begin{aligned} |m(t)|^2 &= 1 + \beta + 2\sqrt{\beta} \cdot \cos(2\pi \Delta f t - \theta) \\ &= 1 + \beta + 2\sqrt{\beta} \cdot \cos\left[2\pi \Delta f (t - \tau)\right] \end{aligned} \quad (2)$$

where $\theta = (\tau/T_0) \cdot 2\pi$, in which $T_0 = 1/\Delta f$ is the cosine waveform period, and τ is the cosine waveform temporal delay. Clearly, the spectral phase difference θ between the two spectral lines is directly related to the temporal phase of the cosine waveform, which, in turn, is directly related to the measurable quantity of the cosine waveform temporal delay τ. After all the spectral phase differences have been measured by filtering adjacent pairs of spectral lines consecutively, the whole set of spectral phases can be obtained by simply cascading all the phase differences. The spectral intensity can be measured separately using an optical spectrum analyzer. With the measured spectral intensity and phase, the temporal waveform can be calculated by a Fourier transform. This measurement method can be considered as a line-by-line version of those demonstrated in [19] and [20].

To show both the accuracy of the phase profile applied by the pulse shaper and the accuracy of the measurement method, first, we use just the second (characterization) pulse shaper. The second pulse shaper simultaneously selects two lines and applies a phase shift on one of the lines. We then measure the temporal delay. Fig. 4(a) shows the spectrum with two lines selected in both linear scale and log scale (inset) and the laser running at 10.0 GHz repetition rate. The two lines are equalized to have the same height, which is made possible by the accurate intensity control afforded by the pulse shaper. Compared with previous pulse measurements using this method [16], one important improvement is that the undesired lines are almost completely suppressed (higher than 35 dB suppression ratio in this example—undesired lines are buried in the noise background). This is a direct consequence of the high resolution of our pulse shaper. Such high suppression ratio is critically important to avoid distortion of the cosine waveform and thus accurate determination of temporal delay [16]. Fig. 4(b) shows the intensity profiles of waveforms in the time domain by applying different phase shifts on one of the lines—detected by a 50-GHz photodiode and measured by a sampling oscilloscope (averaged 20 times). All four waveforms, indeed, show a cosine function with a temporal delay determined by the applied phase shift according to (2) [9]. With respect to the cosine waveform without phase shift (0-ps delay), the ideal relative delays should be 25, 50, and 75 ps, corresponding to $\pi/2$, π, and $3\pi/2$ relative

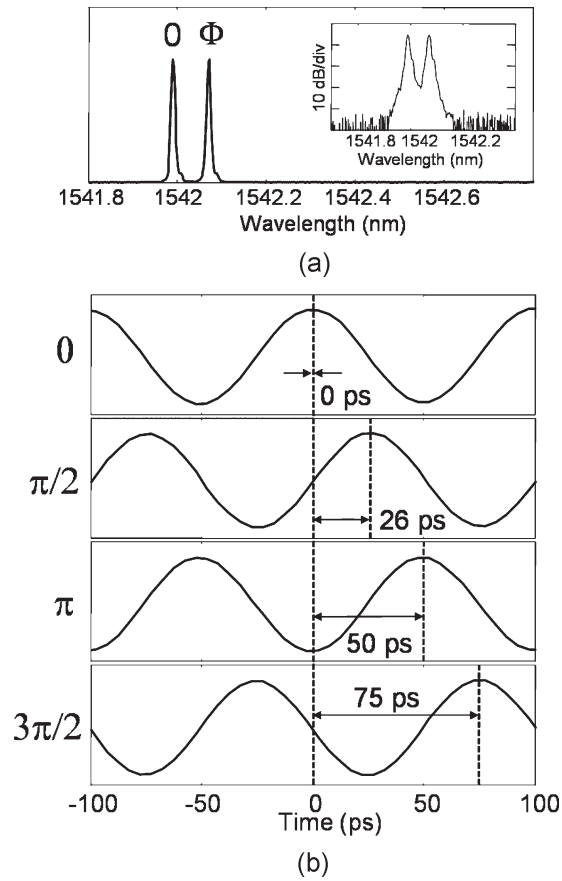

Fig. 4. (a) Two spectral lines selected. (b) Sampling scope traces with phase modulation (0, $\pi/2$, π, and $3\pi/2$) on one spectral line. The traces are the average of 20 measurements.

phase shifts (considering the 100-ps period). The measured values are 26, 50, and 75 ps, respectively, almost perfectly agreeing with the ideal values. The measurement accuracy is limited by the sampling scope, which has a timing step size of 1 ps in our system. From these experiments, we show that both the phase shifts applied by the LCM and the phase measurement using line-by-line control are highly accurate.

In a previous work [12] and in Fig. 4, we have already demonstrated that O-AWG can be achieved with high fidelity after taking great care (including careful intensity/phase calibration of the LCM [2], improved pulse shaper resolution to reduce crosstalk between spectral lines, and matching the spectral line spacing to the pixel spacing). However, spectral phase errors may still occur in practical applications. In such cases, the waveform characterization capability will be critical and should be integrated to the O-AWG functionality for high-fidelity waveform generation. This is similar to the fact that advances in the frontier of short pulse generation benefit significantly from progress in ultrashort pulse measurement techniques. Because the spectral intensity can be monitored by an optical spectrum analyzer, such feedback information would be sufficient to achieve accurate line-by-line intensity control. The difficult part consists of the possible uncertainties in the spectral phases applied to the individual lines, which would significantly affect the temporal waveforms [13]. Therefore, functionalities of both O-AWG and its characterization will be

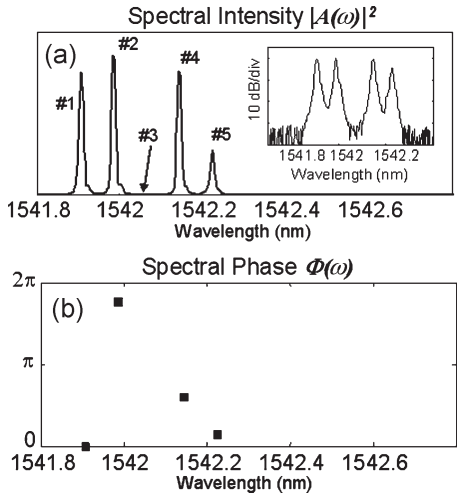

Fig. 5. Five spectral lines with one line missing generated by spectral line-by-line pulse shaping. (a) Spectral intensity measured with an OSA in linear and log scales (inset). (b) Measured spectral phase using spectral line-by-line control.

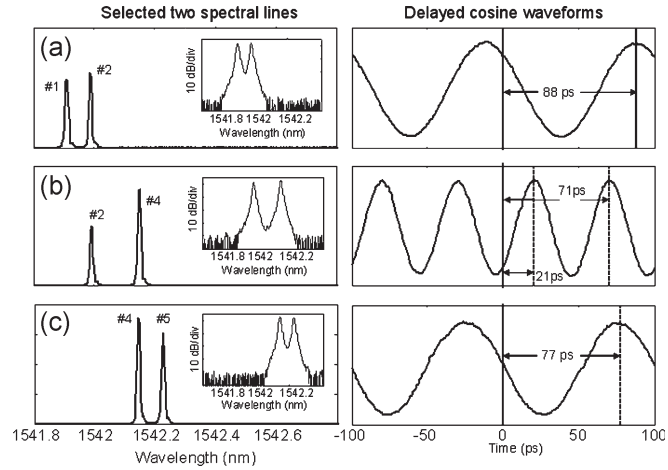

Fig. 6. Two selected spectral lines and corresponding delayed cosine waveforms measured by a sampling scope.

critical to achieve user-specified waveforms with high fidelity. It is clear that the setup in Fig. 2 meets the requirement for both O-AWG and its characterization. Both functions are implemented through spectral line-by-line control, which is especially promising for practical applications.

We now return to experiments using both pulse shapers, one for generation and the other for measurement. Here, we intentionally introduce errors into the generation section to emphasize the importance of the characterization section. For this purpose, we simply mismatch the spectral line spacing and the LCM pixel spacing in the first pulse shaper. In particular, we set the grating incident angle to give an 8.5-GHz optical frequency spacing per LCM pixel, whereas the repetition rate of the laser is set at 10.0 GHz. Such mismatch introduces phase and intensity errors due to the finite beam size of individual spectral lines (some spectral lines will overlap more than one pixel). Note that any other kind of phase error can be monitored exactly in the same way regardless of origin.

In the first example, we generate a waveform corresponding to five spectral lines with one line missing as shown in Fig. 5(a). In addition to the spectral intensity manipulation, the nominal phase profile applied by the first pulse shaper to the selected spectral lines is $[0.30\pi, 0, -, 1.00\pi, 0.40\pi]$. The $-$ symbol is used here to indicate that the spectral line at that position is not present as discussed. The phase errors caused by the aforementioned mismatch are verified by the measurement as shown in Fig. 6. Every pair of two spectral lines is selected by the characterization pulse shaper, and the delay of corresponding cosine waveform is measured. The phase difference between each pair of spectral lines is calculated straightforwardly by (2). For the adjacent two-line pairs (#1 and #2) and (#4 and #5), the cosine period is equal to the period of the mode-locked laser pulses (100 ps). For the two-line pair (#2 and #4) with one line missing, the cosine period is one half the period of the mode-locked laser (50 ps). In this case, the delay τ can be either 21 or 71 ps as shown in Fig. 6(b), which does not affect the phase calculation as it can be performed modulo 2π. By cascading all the measured phase differences between two-line pairs, the spectral phase across the whole spectrum can be obtained as shown in Fig. 5(b), where the spectral phase of the first line is assigned to zero.

The spectral phase of the first line can be specified arbitrarily, which corresponds to a constant phase for the spectrum that is not of interest. The reference point for the delay measurement is also selected arbitrarily, which corresponds to a linear spectral phase across all spectral lines after cascading the phase differences of all two-line pairs [16]. Such linear spectral phase only introduces a timing shift of the temporal waveform that usually is also not of interest. Finally, one may notice that the relative intensities of the selected two-line pair are not the same as those of the original spectral lines. Such an effect does not impact the spectral phase measurement because the delay of the cosine waveform is not related to the relative intensity of the two lines according to (2).

The measured value in Fig. 5(b) is $[0, 1.76\pi, -, 0.60\pi, 0.14\pi]$. To compare it with the nominal value applied by the LCM, we adjust the measured value by adding a constant and linear-ramp phase to the measured values to coincide with the nominal phase value of the first two lines. The adjusted measured phase is $[0.30\pi, 0, -, 0.72\pi, 0.20\pi]$. Compared with the nominally applied values $[0.30\pi, 0, -, 1.00\pi, 0.40\pi]$, the phase errors are significant.

Fig. 7 shows the pulse intensity and phase in the time domain. Solid lines are obtained based on the Fourier transform of the measured spectral intensity and phase. We also measured the pulse intensity using a sampling scope after the 50-GHz photodiode (circles) and using a standard short pulse intensity cross-correlation measurement (diamonds) as shown in Fig. 7(a). The agreement between these three measurements is excellent. Again, the measurement accuracy using line-by-line control is assured by the high-resolution pulse shaper in the characterization section, which exactly selects two spectral lines while almost completely suppressing other spectral lines (this is illustrated by the log scale spectra in the inset of Fig. 6). The waveforms span the full time period as expected for line-by-line pulse shaping. To show the distortions caused by phase errors, the waveforms obtained by Fourier

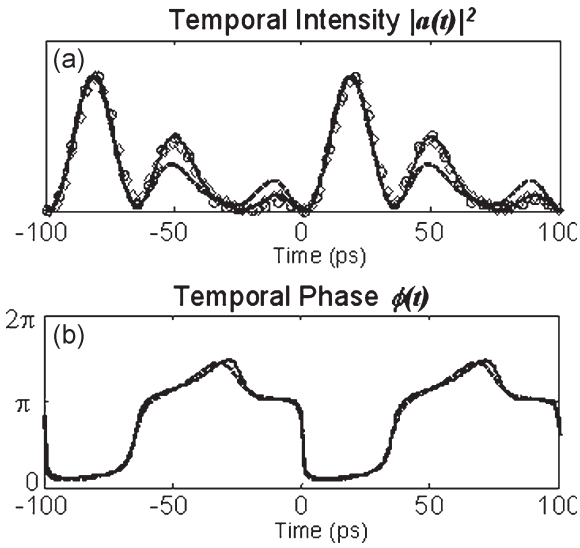

Fig. 7. Waveform (a) temporal intensity and (b) temporal phase corresponding to Fig. 5. Solid lines: Fourier transform of measured spectral intensity and phase. Dashed lines: Fourier transform with nominal spectral phase applied by the LCM. Circles: intensity measured by the sampling scope [only in (a)]. Diamonds: intensity measured by intensity cross correlation [only in (a)]. All the waveforms in (a) are normalized to unity for comparison.

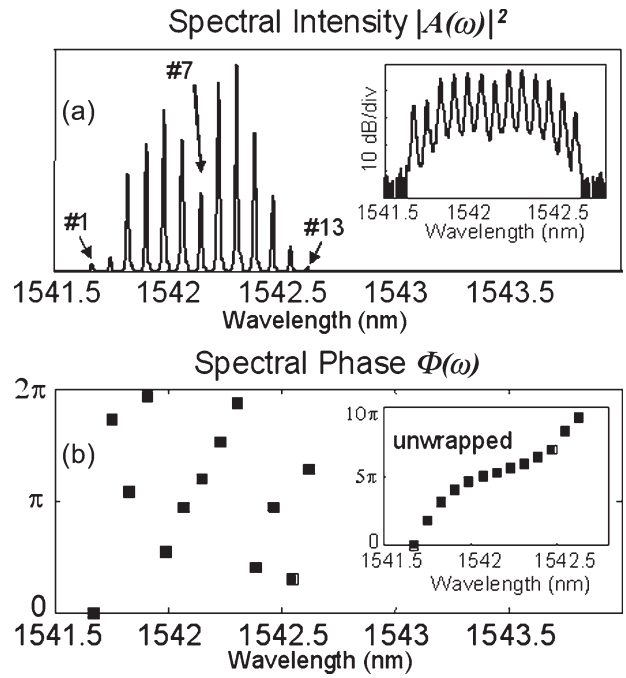

Fig. 8. Thirteen spectral lines with cubic spectral phase generated by spectral line-by-line pulse shaping. (a) Spectral intensity measured with an OSA in linear and log scales (inset). (b) Measured spectral phase using spectral line-by-line control. Inset shows unwrapped spectral phase with cubic characteristics.

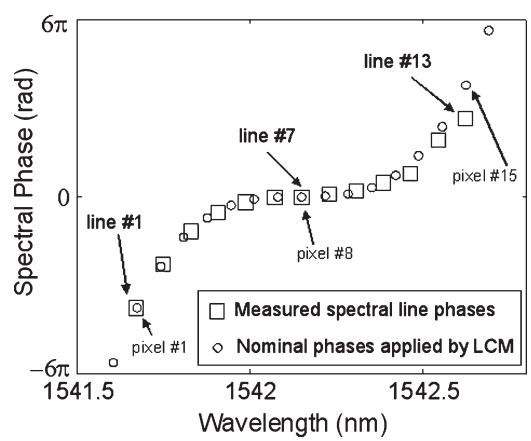

Fig. 9. Comparison between measured spectral phases of 13 lines and the nominal phases corresponding to the 15 pixels of the LCM. The measured spectral phases are adjusted by adding a constant and linear phase onto the unwrapped spectral phases in the inset of Fig. 8(b). The pixel positions are mapped onto the wavelength accordingly.

transform of the measured spectral intensity, but using the nominal spectral phase applied by the LCM, are also plotted (dashed lines). Compared with the other traces, this calculation of the temporal intensity deviates significantly. In this particular case, the difference between the calculated temporal phases is small; nevertheless, this simple example shows that waveform monitoring can play an important role to achieve the desired results in O-AWG.

Fig. 8 shows an example with 13 spectral lines for which the effect of phase errors may be even more prominent. The 13 spectral lines cover around 15 pixels of the generation pulse shaper. Because the mismatch is larger than one pixel, it is impossible to assign the nominal spectral phase applied by the LCM to individual spectral lines. A pure cubic spectral phase in pixel number is applied to the spectral lines by the first pulse shaper, with zero phase shift approximately at the center. However, the actual phase profile as a function of individual spectral line is unknown due to the mismatch. The mismatch can also be noticed from the measured spectral intensity in Fig. 8(a), where some of the spectral lines are attenuated more if they are located between two pixels. This phenomenon results from diffraction effects experienced by the frequency components falling at phase transition regions of the LCM in the pulse shaper. This effect has been treated quantitatively previously [21].

The measured phase profile using line-by-line control in the characterization shaper is plotted in Fig. 8(b). If the phase is unwrapped as shown in the inset, the cubic characteristic is clear. To compare it with the nominal phases applied by the LCM, the measured spectral phases of the 13 lines are adjusted by adding a constant and linear-ramp phase, which is shown in Fig. 9 along with the nominal phases corresponding to the 15 pixels of the LCM. For the nominal phases, the pixel positions are mapped onto wavelength using the known spatial dispersion (8.5 GHz/pixel). The center line (line #7) is assumed to be aligned with the center pixel (pixel #8). The adjusted value of constant and linear phase is chosen such that the center line (line #7) has the same phase shift (zero) as the center pixel (pixel #8) and the leftmost line (line #1) has the same phase shift as pixel #1. As expected, they are similar but with noticeable differences due to the following reasons: 1) The largest discrepancies appear at the right edge. If we adjust phases such that the rightmost line (line #13) has the same phase shift as pixel #15, discrepancies appear at the left edge. 2) The measurement errors using line-by-line control becomes larger at the edges because the selected two lines at the edges have relatively small optical power and thus lower signal-to-noise ratio for the delay measurement. 3) The center line (line #7) is

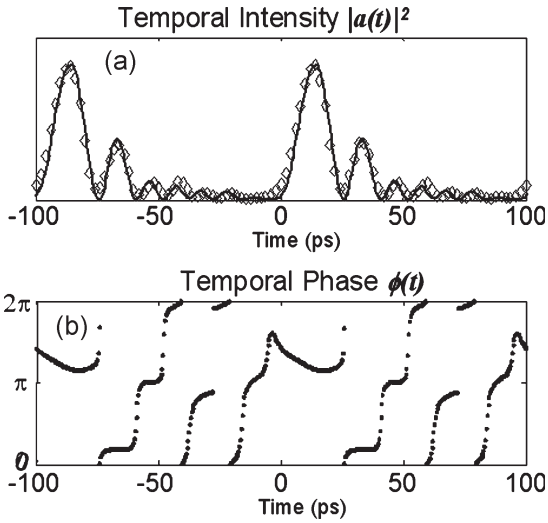

Fig. 10. Waveform (a) temporal intensity and (b) temporal phase corresponding to Fig. 8. Solid lines: Fourier transform of measured spectral intensity and phase. Diamonds: intensity measured by intensity cross correlation [only in (a)].

assumed to be aligned with the center pixel (pixel #8). However, the details of possible slight (less than 1 pixel) frequency offset are unknown.

Fig. 10 shows the pulse intensity and phase in the time domain. Solid lines are obtained based on the Fourier transform of the measured spectral intensity and phase, which agree well with the intensity cross correlation (diamonds) in Fig. 10(a). The temporal intensity shows an oscillatory tail—a property of cubic spectral phase. Again, the waveforms span the full time period as expected. From the point of view of O-AWG, not only is the desired temporal intensity important, but the temporal phase may also need to be tailored in a specified way. In such cases, temporal phase monitoring would be as important as temporal intensity monitoring for O-AWG applications. The temporal phase profile shown in Fig. 10(b) illustrates that such functionality has been automatically included in the current setup.

Accurately determined phases for individual spectral lines could be very valuable feedback information for the first pulse shaper to generate targeted O-AWG signals if any phase errors occur. Usually, the phase errors are small, and the error correction could be simply implemented using a measure-and-correct procedure with a small number of iterations, even without knowledge of the origin of the phase errors.

IV. Conclusion

In summary, we have demonstrated for the first time, to the best of our knowledge, simultaneous optical arbitrary waveform generation and characterization using spectral line-by-line control. User-specified optical waveform is related to the intensity and phase of the spectral lines by a Fourier transform. Complete characterization of O-AWG is important to monitor and thus to improve its performance. With these integrated functionalities, phase errors can be monitored. With appropriate correction procedures, it will be possible to achieve O-AWG with high fidelity even if such errors occur.

Acknowledgment

The authors would like to thank D. S. Seo for his work in constructing the laser.

References

[1] S. T. Cundiff, "Phase stabilization of ultrashort optical pulses," *J. Phys. D, Appl. Phys.*, vol. 35, no. 8, pp. R43–R59, Apr. 2002.

[2] A. M. Weiner, "Femtosecond pulse shaping using spatial light modulators," *Rev. Sci. Instrum.*, vol. 71, no. 5, pp. 1929–1960, May 2000.

[3] Z. Jiang, D. E. Leaird, and A. M. Weiner, "Width and wavelength tunable optical RZ pulse generation and RZ-to-NRZ format conversion at 10 GHz using spectral line-by-line control," *IEEE Photon. Technol. Lett.*, vol. 17, no. 12, pp. 2733–2735, Dec. 2005.

[4] Z. Jiang, D. S. Seo, S.-D. Yang, D. E. Leaird, R. V. Roussev, C. Langrock, M. M. Fejer, and A. M. Weiner, "Four user, 2.5 Gb/s, spectrally coded O-CDMA system demonstration using low power nonlinear processing," *J. Lightw. Technol.*, vol. 23, no. 1, pp. 143–158, Jan. 2005.

[5] J. D. McKinney, D. E. Leaird, and A. M. Weiner, "Millimeter-wave arbitrary waveform generation with a direct space-to-time pulse shaper," *Opt. Lett.*, vol. 27, no. 15, pp. 1345–1347, Aug. 2002.

[6] T. M. Fortier, D. J. Jones, J. Ye, S. T. Cundiff, and R. S. Windeler, "Long-term carrier–envelope phase coherence," *Opt. Lett.*, vol. 27, no. 16, pp. 1436–1438, Aug. 2002.

[7] A. Bartels, N. R. Newbury, I. Thomann, L. Hollberg, and S. A. Diddams, "Broadband phase-coherent optical frequency synthesis with actively linked Ti:sapphire and Cr:forsterite femtosecond lasers," *Opt. Lett.*, vol. 29, no. 4, pp. 403–405, Feb. 2004.

[8] R. Holzwarth, M. Zimmermann, T. Udem, T. W. Hansch, P. Russbuldt, K. Gabel, R. Poprawe, J. C. Knight, W. J. Wadsworth, and P. S. J. Russell, "White-light frequency comb generation with a diode-pumped Cr:LiSAF laser," *Opt. Lett.*, vol. 26, no. 17, pp. 1376–1378, Sep. 2001.

[9] Z. Jiang, D. S. Seo, D. E. Leaird, and A. M. Weiner, "Spectral line-by-line pulse shaping," *Opt. Lett.*, vol. 30, no. 12, pp. 1557–1559, Jun. 2005.

[10] T. Yilmaz, C. M. DePriest, T. Turpin, J. H. Abeles, and P. J. Delfyett, "Toward a photonic arbitrary waveform generator using a modelocked external cavity semiconductor laser," *IEEE Photon. Technol. Lett.*, vol. 14, no. 11, pp. 1608–1610, Nov. 2002.

[11] S. Etemad, T. Banwell, S. Galli, J. Jackel, R. Menendez, P. Toliver, J. Young, P. Delfyett, C. Price, and T. Turpin, "Optical-CDMA incorporating phase coding of coherent frequency bins: Concept, simulation, experiment," presented at the Optical Fiber Conf. (OFC), Los Angeles, CA, 2004, Paper FG5.

[12] Z. Jiang, D. E. Leaird, and A. M. Weiner, "Line-by-line pulse shaping control for optical arbitrary waveform generation," *Opt. Express*, vol. 13, no. 25, pp. 10431–10439, Dec. 2005.

[13] R. Trebino, *Frequency-Resolved Optical Gating: The Measurement of Ultrashort Laser Pulses*. Norwell, MA: Kluwer, 2004.

[14] C. Iaconis and I. A. Walmsley, "Spectral phase interferometry for direct electric-field reconstruction of ultrashort optical pulses," *Opt. Lett.*, vol. 23, no. 10, pp. 792–794, May 1998.

[15] C. Dorrer and I. Kang, "Complete temporal characterization of short optical pulses by simplified chronocyclic tomography," *Opt. Lett.*, vol. 28, no. 16, pp. 1481–1483, Aug. 2003.

[16] P. Kockaert, M. Peeters, S. Coen, P. Emplit, M. Haelterman, and O. Deparis, "Simple amplitude and phase measuring technique for ultrahigh-repetition-rate lasers," *IEEE Photon. Technol. Lett.*, vol. 12, no. 2, pp. 187–189, Feb. 2000.

[17] P. Kockaert, M. Haelterman, P. Emplit, and C. Froehly, "Complete characterization of (ultra)short optical pulses using fast linear detectors," *IEEE J. Sel. Topics Quantum Electron.*, vol. 10, no. 1, pp. 206–212, Jan./Feb. 2004.

[18] P. Kockaert, J. Azana, L. R. Chen, and S. LaRochelle, "Full characterization of uniform ultrahigh-speed trains of optical pulses using fiber Bragg gratings and linear detectors," *IEEE Photon. Technol. Lett.*, vol. 16, no. 6, pp. 1540–1542, Jun. 2004.

[19] J. P. Heritage, A. M. Weiner, and R. N. Thurston, *Ultrafast Phenomena V*. Berlin, Germany: Springer-Verlag, 1986, pp. 34–37.

[20] K. C. Chu, J. P. Heritage, R. S. Grant, K. X. Liu, A. Dienes, W. E. White, and A. Sullivan, "Direct measurement of the spectral phase of femtosecond pulses," *Opt. Lett.*, vol. 20, no. 8, pp. 904–906, Apr. 1995.

[21] R. N. Thurston, J. P. Heritage, A. M. Weiner, and W. J. Tomlinson, "Analysis of picosecond pulse shape synthesis by spectral masking in a grating pulse compressor," *IEEE J. Quantum Electron.*, vol. QE-22, no. 5, pp. 682–696, May 1986.

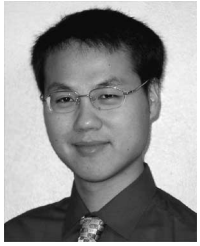

Zhi Jiang (S'03) received the B.S. (with highest honors) and M.S. degrees in electronics engineering from Tsinghua University, Beijing, China, in 1999 and 2002, respectively. He is currently working toward the Ph.D. degree in electrical and computer engineering at Purdue University, West Lafayette, IN.

His research focuses on the areas of ultrafast technology, optical pulse shaping, optical fiber communication, and fiber nonlinearity.

Mr. Jiang received the Ross and Mary I. Williams Fellowship, Purdue University, in 2002–2003. He has been selected as a finalist for the 2005 OSA New Focus/Bookham Student Award. He is one of the recipients of the 2005 IEEE/LEOS Graduate Student Fellowships.

Daniel E. Leaird (M'01–SM'05) was born in Muncie, IN, in 1964. He received the B.S. degree in physics from Ball State University, Muncie, in 1987 and the M.S. and Ph.D. degrees in electrical and computer engineering from Purdue University, West Lafayette, IN, in 1996, and 2000, respectively.

He joined Bell Communications Research (Bellcore), Red Bank, NJ, as a Senior Staff Technologist in 1987 and later advanced to member of Technical Staff. From 1987 to 1994, he was with the Ultrafast Optics and Optical Signal Processing Research Group, where he was a key Team Member in research projects in ultrafast optics, such as shaping of short optical pulses using liquid crystal modulator arrays, investigation of dark soliton propagation in optical fibers, impulsive stimulated Raman scattering in molecular crystals, and all-optical switching. He has been with Purdue University since 1994 and is currently a Senior Research Scientist and Laboratory Manager of the Ultrafast Optics and Optical Fiber Communications Laboratory in the School of Electrical and Computer Engineering. He is also serving as a Consultant to venture capitalists by performing technical due diligence. He also serves as a frequent Reviewer for *Optics Letters*, *Optics Express*, *Photonics Technology Letters*, *Applied Optics*, and the *Journal of the Optical Society of America B*, in addition to serving on the National Science Foundation review panels in the SBIR program. He has coauthored approximately 60 journal articles, 80 conference proceedings, and two U.S. patents.

Dr. Leaird is active in the optics community and professional organizations including the Optical Society of America and the IEEE Lasers and Electro-Optics Society (LEOS), where he is a member of the Ultrafast Technical Committee. He has received several awards for his work in the ultrafast optics field including a Bellcore "Award of Excellence," a Magoon Award for outstanding teaching, and an Optical Society of America/New Focus Student Award.

Andrew M. Weiner (S'84–M'84–SM'91–F'95) received the Sc.D. degree in electrical engineering from the Massachusetts Institute of Technology (MIT), Cambridge, in 1984.

From 1979 to 1984, he was a Fannie and John Hertz Foundation Graduate Fellow with MIT. Upon graduation, he joined Bellcore as a Member of Technical Staff and was promoted to Manager of Ultrafast Optics and Optical Signal Processing Research. In 1992, he moved to Purdue University, West Lafayette, IN, where he served as the ECE Director of Graduate Admissions from 1997 to 2003 and is currently the Scifres Distinguished Professor of electrical and computer engineering. He pioneered the field of femtosecond pulse shaping, which enables the generation of nearly arbitrary ultrafast optical waveforms according to user specification. He has published five book chapters and over 175 journal articles. He has been an author or coauthor of over 300 conference papers, including approximately 80 conference invitational talks, and has presented over 70 additional invitational seminars at university, industry, and government organizations. He is also the holder of eight U.S. patents. His research interests include ultrafast optical signal processing and high-speed optical communications.

Dr. Weiner was the recipient of numerous awards, including the Hertz Foundation Doctoral Thesis Prize (1984), the Adolph Lomb Medal of the Optical Society of America (1990), the Curtis McGraw Research Award of the American Society of Engineering Education (1997), the International Commission on Optics Prize (1997), the IEEE LEOS William Streifer Scientific Achievement Award (1999), the Alexander von Humboldt Foundation Research Award for Senior U.S. Scientists (2000), and the inaugural Research Excellence Award from the College of Engineering, Purdue University (2003). He has served as Co-Chair of the Conference on Lasers and Electro-optics and the International Conference on Ultrafast Phenomena and as an Associate Editor of several journals. He has also served as Secretary/Treasurer of IEEE LEOS and as Vice-President of the International Commission on Optics. He is a Fellow of the Optical Society of America.